

High Resolution Observations and Numerical Simulations of Chromospheric Fibrils and Mottles

Bart De Pontieu¹, Viggo H. Hansteen², Luc Rouppe van der Voort²,
 Michiel van Noort³ and Mats Carlsson,²

¹*Lockheed Martin Solar and Astrophysics Lab, Palo Alto, CA, USA*

²*Institute of Theoretical Astrophysics, University of Oslo, Norway*

³*Institute for Solar Physics of the Royal Swedish Academy of Sciences,
 Sweden*

Abstract. With the recent advent of the Swedish 1-m Solar Telescope (SST), advanced image processing techniques, as well as numerical simulations that provide a more realistic view of the chromosphere, a comprehensive understanding of chromospheric jets such as spicules, mottles and fibrils is now within reach. In this paper, we briefly summarize results from a recent analysis of dynamic fibrils, short-lived jet-like features that dominate the chromosphere (as imaged in $H\alpha$) above and about active region plage. Using extremely high-resolution observations obtained at the SST, and advanced numerical 2D radiative MHD simulations, we show that fibrils are most likely formed by chromospheric shock waves that occur when convective flows and global oscillations leak into the chromosphere along the field lines of magnetic flux concentrations.

In addition, we present some preliminary observations of quiet Sun jets or mottles. We find that the mechanism that produces fibrils in active regions is most likely also at work in quiet Sun regions, although it is modified by the weaker magnetic field and the presence of more mixed-polarity. A comparison with numerical simulations suggests that the weaker magnetic field in quiet Sun allows for significantly stronger (than in active regions) transverse motions that are superposed on the field-aligned, shock-driven motions. This leads to a more dynamic, and much more complex environment than in active region plage. In addition, our observations of the mixed polarity environment in quiet Sun regions suggest that other mechanisms, such as reconnection, may well play a significant role in the formation of some quiet Sun jets. Simultaneous high-resolution magnetograms (such as those provided by Hinode), as well as numerical simulations that take into account a whole variety of different magnetic configurations, will be necessary to determine the relative importance in quiet Sun of, respectively, the fibril-mechanism and reconnection.

1. Introduction

Spicules and related flows such as mottles and fibrils dominate the highly dynamic chromosphere (Rutten, 2007, this volume), a region in which over 90% of the non-radiative energy going into the outer atmosphere to drive solar activity and space weather is deposited. Spicules are relatively thin, elongated structures, best seen at the limb in $H\alpha$. They are but one form of the many “spicular” features that dominate the chromosphere, such as quiet Sun mottles, or active region (AR) fibrils, both observed on the disk (Beckers 1968). Even

though it is not clear how all of these “spicular features” are related, it seems that all represent real mass motion of chromospheric plasma to coronal heights (see, e.g., the many EUV absorbing features in images taken with the Transition Region and Coronal Explorer, TRACE, Handy et al. 1999).

Spicules (at the limb), mottles (on the quiet Sun disk) and fibrils (in active regions) have been studied for many decades, but until recently they have remained poorly understood, because of a lack of high quality observations: their diameters of a few hundred km and lifetimes of a few minutes were too close to observational limits. In addition, theoretical models were usually highly simplified (1D) and focused mainly on spicule-like jets in isolation from the surrounding, driving atmosphere. Several recent advances have now enabled major breakthroughs in our understanding of at least some of these dynamic chromospheric jets.

On the observational side, new telescopes such as the Swedish 1 m Solar Telescope (SST, Scharmer et al. 2003) in La Palma, as well as advanced image processing techniques, such as the Multi-Object Multi-Frame Blind Deconvolution method (MOMFBD, van Noort et al. 2005), have allowed diffraction-limited (~ 120 km) time series in chromospheric lines (e.g., $H\alpha$) at extremely high temporal resolution (1 second). These datasets have, for the first time, resolved the dominant temporal and spatial evolution of active region fibrils and quiet Sun mottles (Hansteen et al. 2006; De Pontieu et al. 2007).

Parallel to these observational advances, theoretical efforts have also made significant progress. Several papers have explored, for the first time, the intricate relationship between the formation of fibrils and the photospheric magnetoconvective flowfield. De Pontieu et al. (2004) used a synthesis of idealized 1D modeling and observations to propose that photospheric oscillations can leak into the chromosphere, where they form shocks to drive fibrils upwards. This idea was based on the close connection between oscillations in upper transition region moss (De Pontieu et al. 1999) and the presence of quasi-periodic jets or fibrils in the chromosphere above active region plage (De Pontieu et al. 2003a). These ideas have now been confirmed and expanded by Hansteen et al. (2006) and De Pontieu et al. (2007) who analyzed a diffraction-limited time series of $H\alpha$ fibrils, and directly compared them to advanced radiative MHD simulations. They find excellent agreement between observations and simulations.

In this paper, we will very briefly summarize the analysis of Hansteen et al. (2006) and De Pontieu et al. (2007) in Section 2. While this analysis explains the formation of fibrils above active region plage, it is not yet fully clear what role this mechanism plays in quiet Sun. To explore this issue, we show (in Section 3) some very preliminary results of an analysis of very recent SST observations of the quiet Sun chromosphere.

2. Active Region Fibrils

Hansteen et al. (2006) and De Pontieu et al. (2007) use $H\alpha$ observations with 120 km spatial resolution and 1 s temporal resolution to study the evolution of so-called dynamic fibrils (DFs). These fibrils are relatively short (1,250 km on average), thin (120-700 km) and jet-like features that occur above or in the direct vicinity of active region plage. They are the same jets that dominate the dynam-

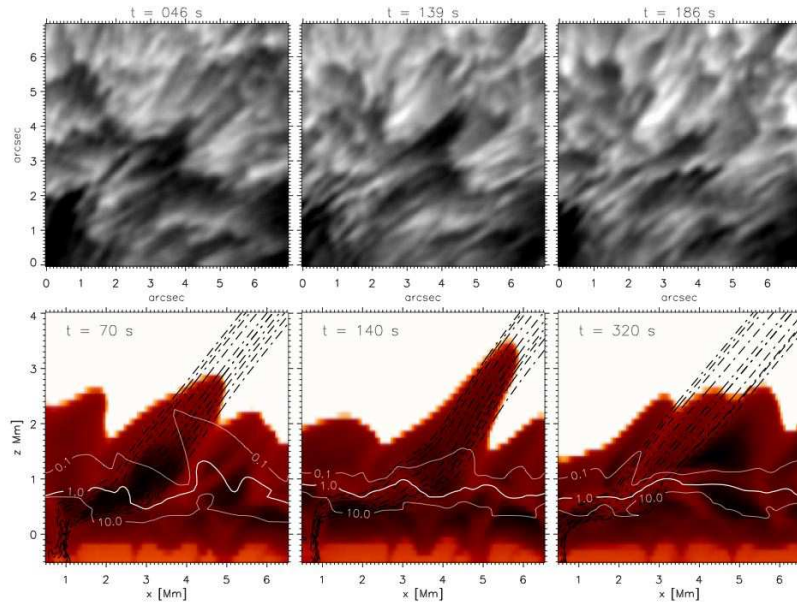


Figure 1. Taken from Hansteen et al. (2006). Temporal evolution of dynamic fibrils from $H\alpha$ linecenter observations at the SST (top panels), and from numerical simulations (bottom panels). The observations show a dark elongated feature with an upper chromospheric temperature of less than 10,000 K rise and fall within 4 minutes. Its maximum length is about 2 arcseconds. The bottom panels show the logarithm of the plasma temperature T , which is set to saturate at $\log T = 4.5$, from numerical simulations covering the upper convection zone ($z < 0$) up through the corona (white region at the top). The vertical scale has its origin at the photosphere (where the optical depth $\tau_{500} = 1$). Contours of plasma β are drawn in white where $\beta = 0.1, 1, 10$. The simulations show that dynamic fibrils ascend as a result of upwardly propagating shock waves. These shock waves seem to preferentially enter the corona where the magnetic field lines (dotted black lines) also enter the corona.

ics on timescales of minutes of the upper TR moss emission (De Pontieu et al. 2003b). Extensive statistical analysis of the $H\alpha$ timeseries reveals that most dynamic fibrils have short lifetimes of 3 to 6 minutes, with clear differences in lifetimes depending on the magnetic topology of the plage region. Plage regions with more vertically oriented field are dominated by DFs with lifetimes of 3 minutes, whereas less dense plage region or plage where the field is more inclined from the vertical typically show DF lifetimes of order 5 minutes. Note that what are traditionally called $H\alpha$ fibrils typically includes a large subset of almost horizontal loops that form a canopy-like structure that connects neighboring plage regions or sunspots. This subset of usually much longer fibrils is clearly more stable (in time) than the DFs. Wavelet analysis shows that whereas the DFs are dominated by quasi-period oscillations with periods that are identical to the DF lifetimes (i.e., 3 and 5 mins), the horizontal fibrils show quasi-periodicity with periods longer than 10 minutes (Hansteen et al. 2006; De Pontieu et al. 2007).

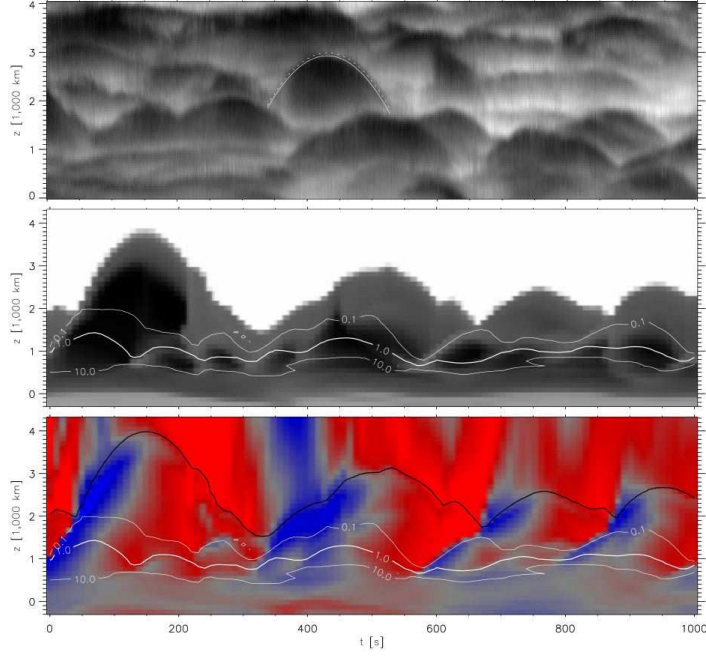


Figure 2. Taken from Hansteen et al. (2006). Space-time plots of: the height of dynamic fibrils for $H\alpha$ linecenter observations (top panel), the logarithm of the plasma temperature in numerical simulations (middle panel), and simultaneous plasma velocity from the same simulation (bottom panel). Most of the dynamic fibrils in the top panel follow a near perfect parabolic path in their rise and descent from the lower atmosphere. Parabolic paths with similar parameters are traced by fibril-like features in the 2D numerical simulations (middle panel). Contours of plasma β are drawn in white where $\beta = 0.1, 1, 10$. Upward plasma velocities (blue in the bottom panel) show the upward propagation of the shocks that drive the fibril-like features along their parabolic path. This initial upward impulse is followed by a constant deceleration which leads to downward velocities (red) of roughly equal magnitude as the initial upward velocities. The black line in the bottom panel outlines the top or transition region of the simulated chromospheric fibrils.

One of the major findings of Hansteen et al. (2006) and De Pontieu et al. (2007) is that almost all fibrils that can be nicely isolated from the background or foreground of other fibrils, follow an almost perfect parabolic path in their ascent and descent (Figs. 1, 2). The sharp delineation of the fibril tops is presumably related to the fact that these fibrils have sharp transition regions at their top end. The measurements thus trace the path of the transition region. The velocity of the TR at the beginning of a fibril's life is between 10 and 35 km/s (projected), i.e., supersonic speeds. The velocity then linearly decreases with time, reverses sign and, at the end of the fibril's life, reaches a maximum speed that is similar in magnitude as the initial speed. The deceleration fibrils undergo is significantly less than solar gravity, ranging from 50 to 300 m/s². Fibrils typically have internal structure, with various parts rising and falling with slightly different

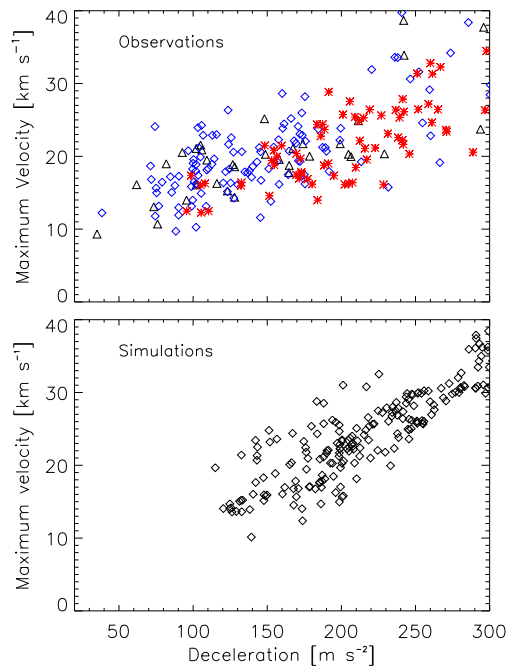


Figure 3. Adapted from Hansteen et al. (2006). Decelerations have been corrected by a factor of 2 (see De Pontieu et al. (2007) for details). Maximum velocities versus decelerations from 257 observed dynamic fibrils (top panel). The maximum velocity and deceleration have been corrected for line-of-sight projection, assuming that the fibril is aligned with the local magnetic field as deduced from potential field calculations. Red stars indicate fibrils from the dense plage region, whereas blue diamonds indicate fibrils in the inclined field region. The same scatterplot (lower panel), made from analyzing fibril-like features in the numerical simulations, reveals that the simulations reproduce the observed correlation between these parameters, as well as reproducing the range in deceleration and maximum velocity.

speeds and decelerations. The widths mentioned above were defined as the width over which the parabolic paths still look similar in lifetime and speed.

The numerical simulations described in Hansteen et al. (2006) and De Pontieu et al. (2007) show that fibril-like features occur in a natural fashion in the proximity of flux concentrations, as a result of chromospheric shocks. These shocks form when convective flows and oscillations leak into the chromosphere along magnetic field lines. Figure 1 shows that the jet-like features formed in the simulations have lengths and lifetimes that are similar to the observed fibrils. The simulations also show that the parabolic paths observed in $H\alpha$ fibrils are a clear sign that these jets are caused by single slow-mode magneto-acoustic shocks. This is evident from Fig. 2, where the shocks are clearly seen in the xt -plot of the velocity in the simulations (bottom panel). One of the most striking results is that the jet-like features in the simulation not only reproduce the parabolic paths, but also the observed correlations between the deceleration and maximum velocity (Fig. 3).

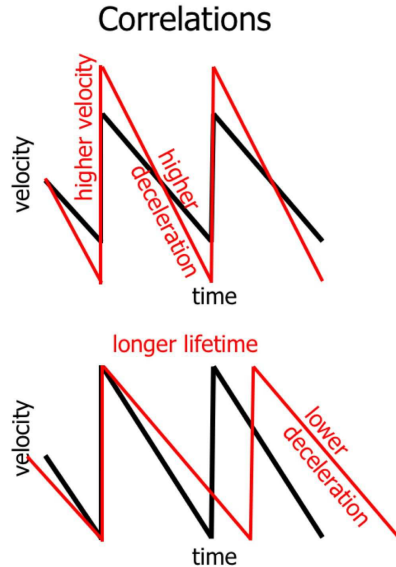


Figure 4. Cartoon illustrating the cause for the correlations between the deceleration and maximum velocity of fibrils (see Fig. 3), and between lifetime and maximum velocity of fibrils (see De Pontieu et al. 2007). Given a fixed lifetime (or shock wave period), higher velocity amplitudes automatically lead to higher decelerations. For a fixed velocity amplitude, longer wave periods lead to lower decelerations.

This correlation can be understood in terms of shock wave physics, as illustrated in Fig. 4. Preliminary results of a parameter study of detailed numerical simulations indicate that this intuitive explanation does indeed dominate the observed correlation between velocity and deceleration (Hegglund, De Pontieu, Hansteen, in preparation).

Hansteen et al. (2006) and De Pontieu et al. (2007) find clear differences in fibril properties for two different plage regions. They find higher decelerations, slightly lower velocities, shorter lifetimes and shorter lengths for a dense plage region where the magnetic field is inclined more vertically. In a neighboring plage region, where the field is more inclined from the vertical they find fibrils with lower decelerations, slightly higher velocities, longer lifetimes and longer lengths. All of these measurements are of course projected onto the plane of the sky, which potentially leaves the possibility that these differences are caused by projection effects. While Hansteen et al. (2006) and De Pontieu et al. (2007) use magnetic field extrapolations to exclude this possibility, a more straightforward consideration directly shows that the regional differences are not caused by projection effects, but are rather a sign of real physical differences between the two regions. Let us consider whether there exists a viewing angle that would cause all differences to disappear between both regions. This is clearly impossible, for two reasons. Firstly, the lifetimes are very different between both regions. Lifetimes are very well defined, and independent of viewing angle. Secondly, let

us assume a difference in viewing angle is causing the other differences. Assume that the dense plage region is more tilted towards the observer than the other plage region. In such a case the projected lengths, velocities and decelerations would be lower than those measured along the axis of the fibril. In other words, such a viewing angle difference could resolve the difference in lengths and velocity, but would render the difference in deceleration even worse than it already is. This shows that projection effects cannot explain these differences. In addition, the correlations between various parameters that were found are also independent of projection angle, since both parameters would be corrected by the same factor.

The fact that fibrils are caused by single shock waves is apparently confirmed by the work of Langangen et al. (this volume), who use $H\alpha$ spectra from the SST to determine velocities and decelerations of dynamic fibril features. Similar shock-like features also seem to be present in the data presented by Cauzzi et al. (this volume), although further analysis is necessary to confirm this.

Future work will need to involve more advanced radiative transfer calculations for $H\alpha$ in the numerical simulations. Such calculations could provide insight into why the horizontal fibrils are generally not as dynamic as the DFs, and whether the fact that those fibrils are along loops that most often do not have a transition region plays an important role in its more stable behavior.

3. Quiet Sun Mottles

Preliminary analysis of data from 18-June-2006 shows that the quiet Sun chromosphere as imaged in a diffraction-limited, 5 s cadence $H\alpha$ linecenter timeseries, is much more complex than similar timeseries for active regions. The more complex topology of the quiet Sun with its predominantly mixed polarity magnetic fields leads to a much more diverse appearance of dark and bright features (see Fig. 5). Active regions are dominated by long horizontal fibrils and short dynamic fibrils. Quiet Sun has equivalent features: long horizontal dark mottles and short dynamic mottles, that both connect to network regions. In addition, quiet Sun shows many short, highly curved and highly dynamic features that do not seem to be associated with network, but mostly appear in the internetwork (see the area around $21''$, $4''$ in Fig. 5). These internetwork features can often be seen underneath the canopy-like long horizontal mottles, so they seem to be formed at lower heights than the “canopy”. The internetwork features seem to be associated with the underlying granular dynamics. In this section we will focus on the network-associated features.

Contrary to active regions, it is generally extremely difficult to track single QS mottles during their lifetime. One reason for this difficulty is that many mottles lack the sharp “top” end that dominates the appearance of dynamic fibrils in active regions. More importantly, most mottles undergo not only up and downward motions along the direction of the magnetic field, but also significant motions transverse to the magnetic field, as well as fading or dimming during their lifetime. The transverse motions are often well organized or coherent over several arcseconds, so that a whole batch of almost parallel mottles seem to undergo rocking or rotating motions during their lifetime. The apparently changing (with time) opacity as well as the transverse motions often lead to

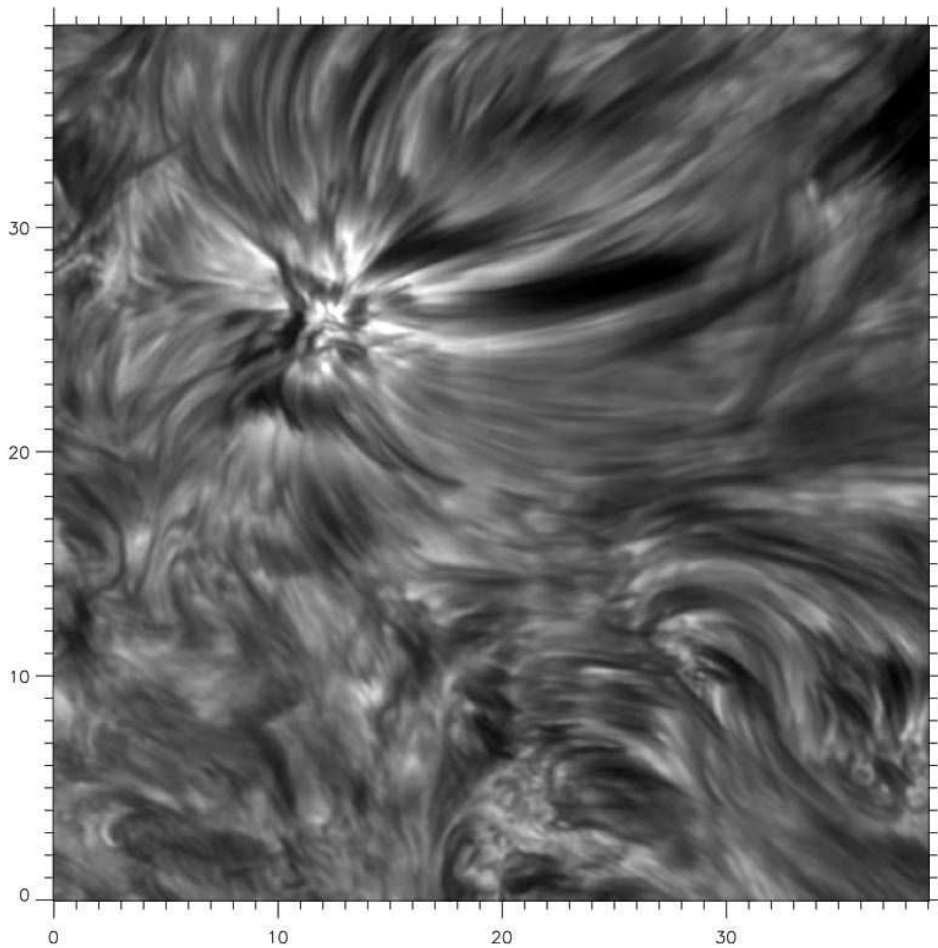


Figure 5. Diffraction-limited image taken at the SST on 18-June-2006 showing H α linecenter of a quiet region. Note the long and curved dark mottles emanating from a network region around (10'', 25''). When tracing loops from the network region to the upper right, a pattern below the loops becomes visible because of lower opacity in the loops. This is the same pattern that is visible in the internetwork regions that are visible in the lower left of the image.

line-of-sight superposition, which renders unique identification throughout the lifetime of the mottle often quite challenging. Figure 6 shows an example of the transverse motion a short mottle (associated with network) undergoes. While its top end is initially at (1'', 1.7''), the whole mottle moves to the lower right, and the top ends at (1.7'', 1.1'') after 51 seconds. The average speed transverse to the mottle axis is of order 13 km/s. Many mottles generally undergo some transverse motion, with typical velocities between 5 and 30 km/s, although larger apparent velocities are also present. It is interesting to note that turning or rotating motions have also been observed in active region fibrils by Koza et

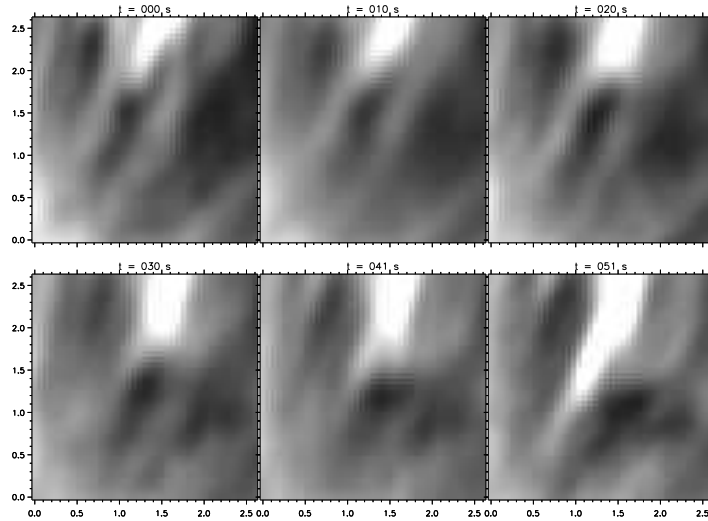


Figure 6. Temporal evolution of a dark mottle that undergoes transverse motions from upper left to lower right. The average velocity with which the mottle is shifted in the direction transverse to its own axis is of order 13 km/s. Units of x and y are in arcseconds.

al. (this volume). We should also note that visual inspection of movies indicates that what appears as a transverse motion may sometimes be an artefact of complicated radiative transfer effects combined with coherent wave-driven motion with phase delay between different (parallel) field lines. For example, it is possible that some apparently transverse motion occurs because brightening and darkening of neighboring field lines is coherent, but with phase delays between neighboring field lines. Such coherence and phase delays would not be surprising, since it has also been observed in active region fibrils (Hansteen et al. 2006; De Pontieu et al. 2007).

Despite the general difficulty with tracing individual mottles, some mottles have a sharply-defined top end and do not show as much transverse motion, so that xt -cuts along the mottle axis can be drawn. In such cases, we find that the mottle top often undergoes a parabolic path, similar to active region fibrils. Several examples are shown in Fig. 7. Why don't all mottles show such parabolic paths? As mentioned, many mottles are not well-defined enough, or move too much in the transverse direction to show a parabolic path in xt -plots. The lack of a well-defined top in many QS mottles is most probably because much of the quiet Sun chromosphere is not in direct thermal contact (along the field line) with a hot transition region. Such contact does occur for dynamic fibrils in active region, so that they do have sharply defined top-ends. It is not a coincidence that most of the well-defined parabolas of Fig. 7 are found in the region directly above or close to the strong network region, where the field is not quite as inclined from the vertical, and coronal loops end. On heavily inclined (i.e., almost horizontal) loops, the mottle tops are not as well defined, presumably because there is no plasma of coronal/TR temperatures anywhere along such loops. Preliminary comparisons with the numerical simulations of

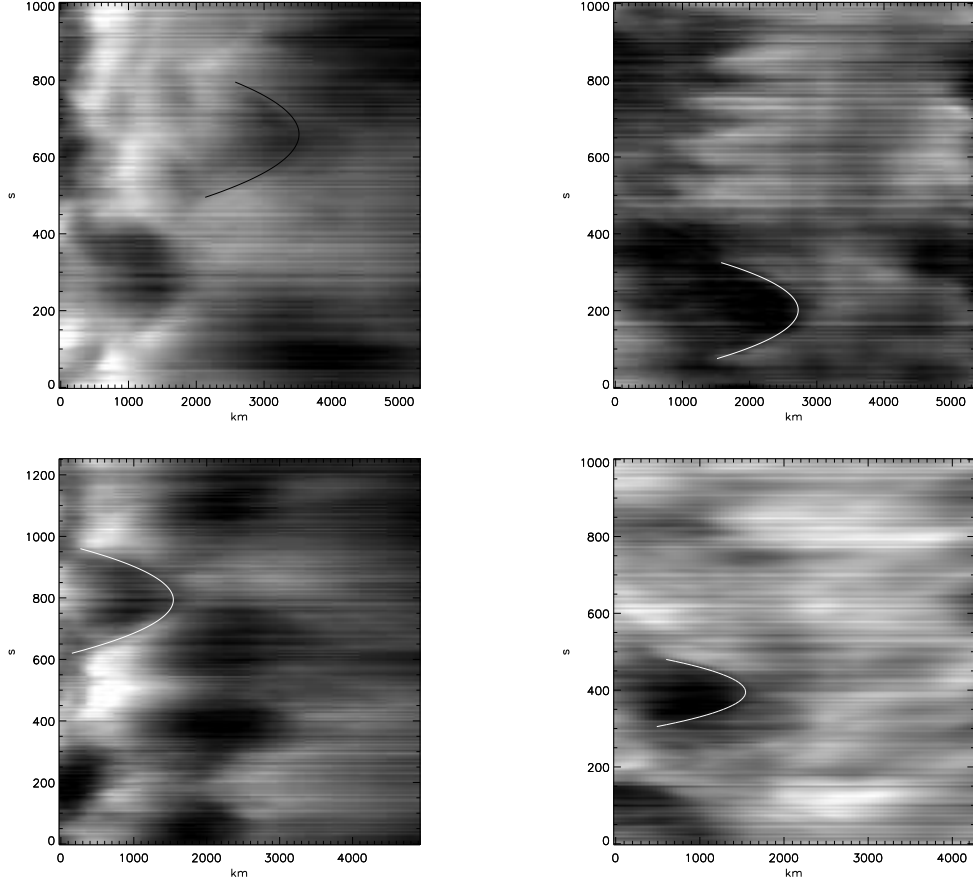


Figure 7. Space-time ('xt') plots of mottles in four different areas, all closely associated with the network at ($10''$, $25''$) of Fig. 5. To mitigate the effects of transverse motion, the xt-plot has been averaged over 10 pixels ($0.53''$) in the direction perpendicular to the mottle axis. While most of the parabolas are not quite as clearly defined as those of fibrils above active region plage, it is clear that parabolic paths occur often for mottles that do not show much transverse motion, and that have a well-defined top. x-axis is in km, y-axis in seconds.

Hansteen et al. (2006) indicate that heavily inclined loops with apex heights less than 2 Mm typically remain chromospheric in temperature from one end to the other end. It is tempting to speculate that on such loops the definition of a mottle top (or end) is no longer determined by the steep temperature increase of the TR (and accompanying steep decrease in opacity), but directly related to the complicated non-LTE line formation of the $H\alpha$ line. Comparisons with detailed $H\alpha$ non-LTE radiative transfer calculations will be necessary to confirm this suspicion.

Regardless of the difficulties of tracking individual mottles, it is clear that many of those that can be tracked follow parabolic paths similar to the paths of active region fibrils. In addition, a preliminary analysis of the correlation

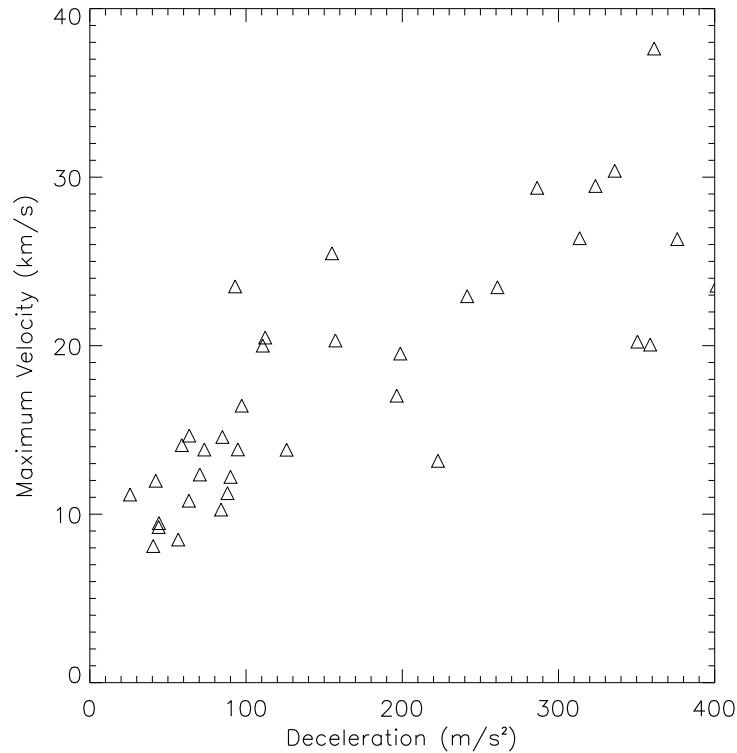


Figure 8. Scatterplot of maximum velocity versus deceleration for 37 quiet Sun mottles. Despite the relatively low statistics, it is clear that a linear correlation similar to the one found for active region fibrils (Fig. 3) is present. A comparison with a similar correlation plot for fibril-like jets in numerical simulations of the chromosphere (bottom panel of Fig. 3) strongly suggests that the fibril-mechanism is also important in the formation of quiet Sun mottles.

between deceleration and maximum velocity of the parabolic paths of quiet Sun mottles (Fig. 8) shows that the deceleration and maximum velocity is linearly correlated. Comparison with Fig. 3 shows that the linear correlation found for quiet Sun mottles is very similar to the one found for active region fibrils, as well as the one found for jets in the numerical simulations. This strongly suggests that the fibril mechanism, i.e., leakage of convective flows and global oscillations into the chromosphere along magnetic field lines, is also important in the formation of jets or mottles in quiet Sun. Note that the minimum velocities are, just like for active region fibrils, around 8 km/s, which is compatible with the chromospheric speed of sound. Such a lower cutoff can be expected since the mottles/fibrils are driven by chromospheric shocks.

Since these results suggest that leakage of global oscillations plays an important role in the dynamics of the quiet Sun chromosphere, we performed a wavelet-based oscillation analysis of two different quiet Sun datasets. The first dataset is a diffraction-limited $H\alpha$ linecenter timeseries taken on 18-June-2006

between 11:54 and 12:42 UT (at 5.15 s cadence). The second dataset is also diffraction-limited, but consists of $H\alpha$ wing images (± 300 mÅ) at 18.4 s cadence, taken on 21-June-2006 between 16:34 UT and 17:28 UT.

A preliminary analysis of the dominant oscillatory behavior of the quiet Sun chromosphere, as imaged in high-resolution $H\alpha$ linecenter timeseries, is shown in Figure 9. This is a map of the dominant wave period for each location of the quiet Sun chromosphere ($H\alpha$ linecenter) that shows significant wavelet power for at least two wave periods. The mottles and loops emanating from the network region around ($25''$, $30''$) are all dominated by oscillatory behaviour with periods around 5-7 minutes, with some of the longer and lower-lying loops dominated by periods of up to 10 minutes. This finding is compatible with the idea that leakage of global oscillations from the photosphere (with dominant periods around 5 minutes) are important in the formation and dynamics of network-associated mottles. The internetwork regions, such as the lower left region, show periods that are closer to 3 minutes. This suggests that internetwork regions (where the field is not as dominant) are dominated by waves with periods around the chromospheric acoustic cutoff period of 3 minutes. It is interesting to note that the 3 min power is also often visible in regions where the long, low-lying loops, e.g. around ($45''$, $45''$), that are typically dominated by longer periods, start to become transparent. This suggests that in such regions lower opacity of the overlying loops allows glimpses of the internetwork dynamics and oscillations underneath.

A similar picture emerges from the $H\alpha \pm 300$ mÅ summed timeseries shown in the upper panels of Fig. 10. The network-associated loops are dominated by periods of 5 min or longer (e.g., around $35''$, $35''$), whereas the internetwork regions (e.g., around $15''$, $25''$) are dominated by 3 minute oscillations. This again strongly suggests that leakage of photospheric oscillations into the chromosphere dominates much of the dynamics of the quiet network chromosphere. There is a hint that right at the center of the network regions, periods closer to 3 minutes appear to occur more often (e.g., at $33''$, $28''$). This is presumably where the field is more vertical, so that the acoustic cutoff period reverts to its nominal 3 min value (similar to the dense plage region in Hansteen et al. (2006)). We also see slightly longer periods dominating the loops connecting two opposite polarity network regions (one centered at $35''$, $30''$, and one at $30''$, $45''$). These longer periods are reminiscent of the periods that are seen in low-lying long fibrils that originate in sunspots or strong plage (De Pontieu et al. 2007). This may not be a coincidence, as the quiet network regions shown here actually contain a stronger than usual amount of magnetic flux (some tiny pores are even visible in the continuum images, not shown).

The dominant periods in the Doppler signal are generally significantly lower than those in the summed signal (bottom panel of Fig. 10). Generally, the areas dominated by 3 min oscillations are a bit more extended in the Doppler signal than in the summed signal, so that the “internetwork” regions cover a larger fraction of the field of view. This may be partially caused by the fact that the overlying canopy is continuously buffeted and impinged by 3 min shocks in the internetwork (similar to the shocks described by Carlsson & Stein (1992, 1994, 1997)), an effect which perhaps starts to dominate the velocity signal at those locations where the canopy becomes more transparent? This could explain why

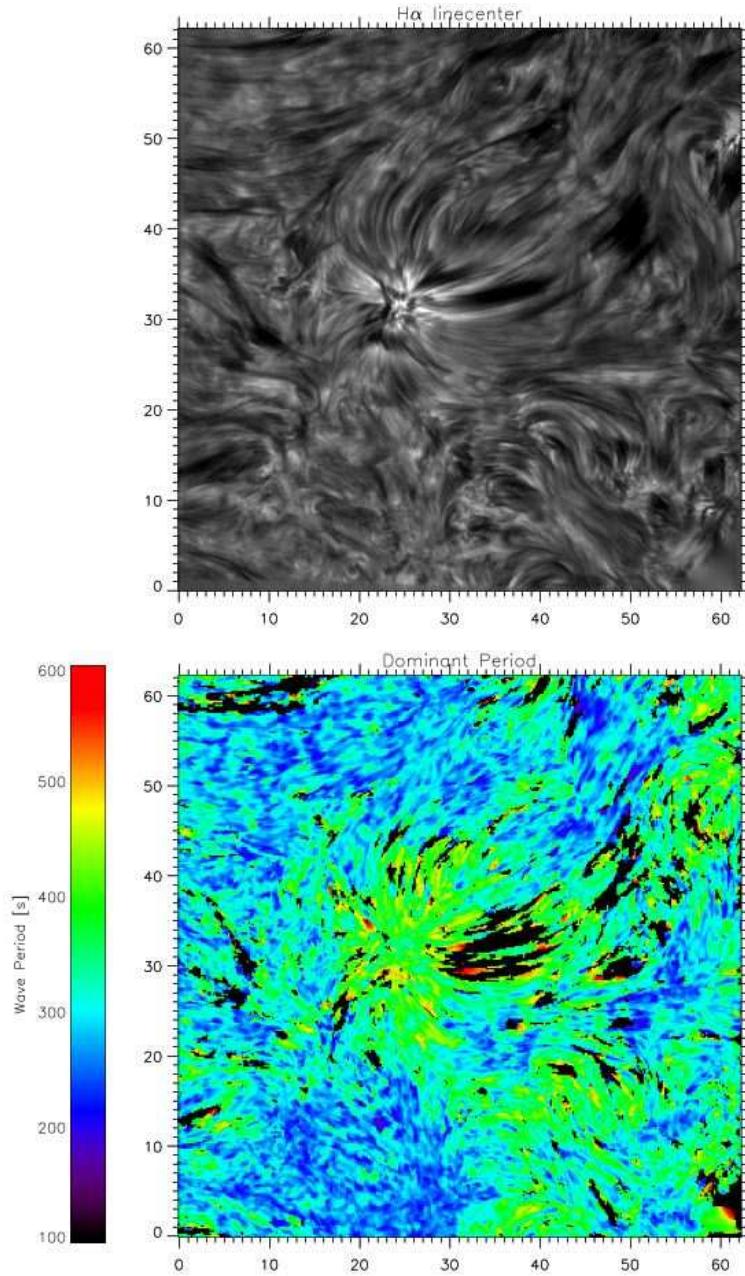


Figure 9. Results from a wavelet analysis of a 48 minute long $H\alpha$ linecenter timeseries of quiet Sun taken on 18-June-2006. The left panel shows a snapshot of the region, whereas the right panel illustrates for each location which wave period dominates, i.e., contains the highest number of wavepackets with significant power.

the influence of the “network” (i.e., 5 min signal) is less spatially extended in the velocity signal than in the intensity signal? Or perhaps the dominant effect is

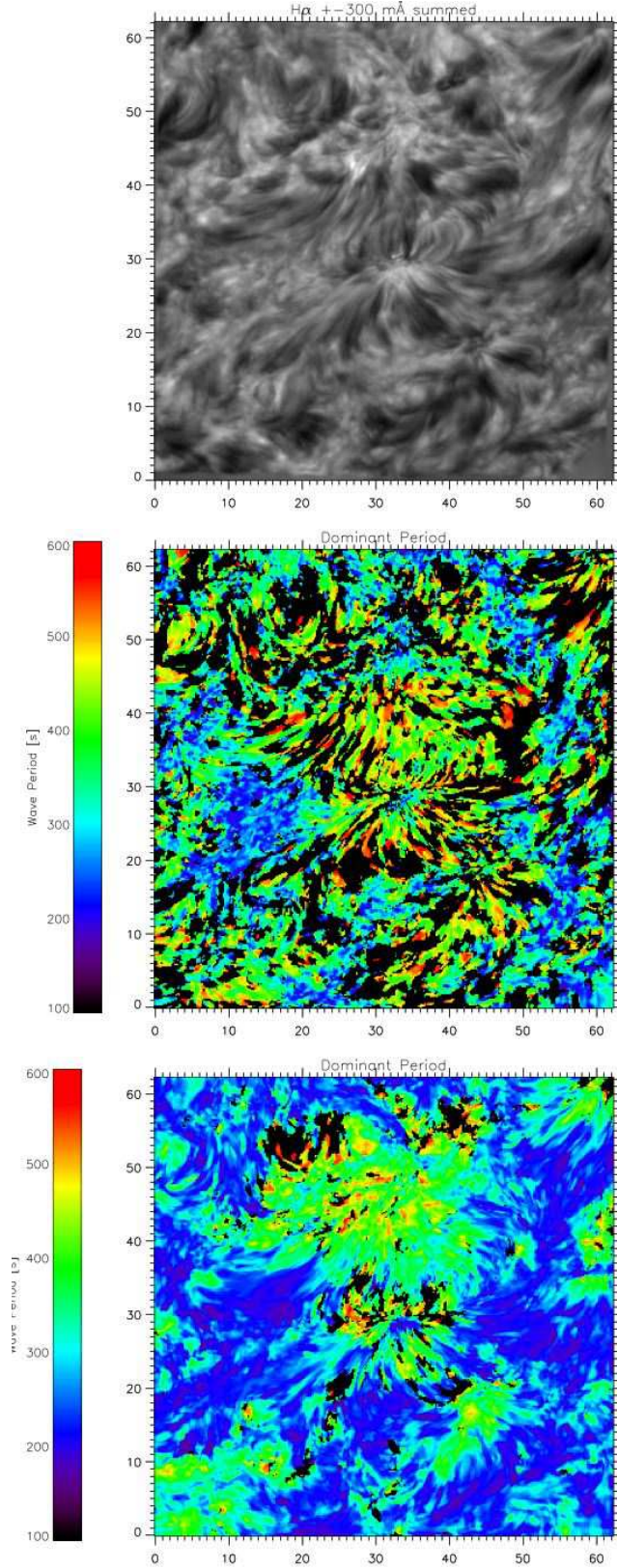


Figure 10. Results from a wavelet analysis of a 54 minute long $H\alpha \pm 300 \text{ m\AA}$ timeseries of quiet Sun taken on 21-June-2006. The top panel shows a snapshot of the region, the middle panel illustrates for each location which wave period dominates in the summed wing images, whereas the bottom panel shows the same for the Doppler signal.

that the velocity signal inherently contains higher frequencies than the intensity signal? The latter is perhaps not surprising since fast-mode magnetoacoustic waves (propagating perpendicular to the field), which predominantly appear in the velocity signal, are ubiquitous in the numerical simulations of Hansteen et al. (2006) and De Pontieu et al. (2007). For example, if fast modes lift a fibril towards the observer along the line-of-sight, such a velocity signal would be completely absent in the intensity signal (which defines the dark mottle). Detailed comparisons with numerical simulations will be necessary to resolve this issue. Such simulations will perhaps also be able to explain why the region around ($30''$, $50''$) is dominated by 3-5 min signals in intensity, and 5-7 min signals in velocity. The region in question is an internetwork region, with little opacity from the overlying canopy (which may be absent altogether at that location). Perhaps the amplitudes in velocity are quite low in this region, so that more long term evolution dominates the signal compared to other internetwork regions?

In concluding, the parabolic paths, correlation between deceleration and maximum velocity and oscillatory properties of quiet Sun mottles strongly suggest that the mechanism that drives active region fibrils is also responsible for the formation of at least a subset of quiet Sun mottles. This is not surprising, since all of the ingredients of the fibril mechanism are also present in quiet Sun: global oscillations and convective flows that are guided into the chromosphere along magnetic field lines. How is this mechanism modified under quiet Sun conditions? The generally weaker magnetic fields of the quiet Sun imply that the height of the plasma $\beta = 1$ surface is generally higher than in active region plage. That implies that the field is less rigid: flows and waves can influence the motion of magnetic field lines up to larger heights. A less rigid field would lead to a much more dynamic magnetic field at upper chromospheric heights, with significantly more transverse motions. This is exactly what we observe in our quiet Sun data. Mode coupling between different wave modes at the plasma $\beta = 1$ surface can also be expected to play a large role in this magnetic environment (Bogdan et al. 2003). In fact, the numerical simulations of Hansteen et al. (2006) and De Pontieu et al. (2007) clearly show that fast-mode magnetoacoustic waves play a significant role in the dynamics of fibril-like jets (under weaker field conditions). These fast modes propagate perpendicular to the fibril-axis, and can lead to a significant transverse motion of the whole fibril-like jet. Our model thus nicely explains the qualitative differences between fibril and mottle dynamics.

Our observations also show many examples where significant reorganizations of the magnetic field occur, with apparent (un?)twisting and motions at Alfvénic speeds. Such reorganizations are most probably signs of magnetic reconnection caused by the dynamic magneto-convective driving of mixed polarity fields in the quiet Sun. While reconnection clearly occurs often in quiet Sun, it is unclear how much of a role reconnection plays in the formation of $H\alpha$ mottles. Taken together with the evidence presented here for a fibril-like mechanism in quiet Sun, it seems quite possible that both reconnection and the shockwave-driven mechanism play a role in jet-formation in quiet Sun. It is possible that one of the reasons the spicule problem has been so difficult to resolve is that there are indeed multiple mechanisms at play, with perhaps a different dominant player for jets observed in different wavelengths (e.g., visual vs. UV). To determine which mechanism dominates where, new datasets (that include si-

multaneous high resolution magnetograms) and more advanced (3D) numerical simulations will be necessary. With the maturing of advanced optics and post-processing techniques, the advent of larger ground-based telescopes and satellite missions (Hinode), as well as more advanced 3D radiative MHD simulations, a solution to these issues is now within reach.

Acknowledgments. BDP thanks the organizers of the meeting for the opportunity to present this work. BDP was supported by NASA grants NAG5-11917, NNG04-GC08G and NAS5-38099 (TRACE), and thanks the ITA/Oslo group for excellent hospitality. VHH thanks LMSAL for excellent hospitality during the spring of 2006. This research was supported by the European Community's Human Potential Programme through the European Solar Magnetism Network (ESMN, contract HPRN-CT-2002-00313) and the Theory, Observation and Simulation of Turbulence in Space (TOSTISP, contract HPRN-CT-2002-00310) programs, by The Research Council of Norway through grant 146467/420 and through grants of computing time from the Programme for Supercomputing. The Swedish 1-m Solar Telescope is operated on the island of La Palma by the Institute for Solar Physics of the Royal Swedish Academy of Sciences in the Spanish Observatorio del Roque de los Muchachos of the Instituto de Astrofísica de Canarias.

References

- Beckers J. M., 1968, *Sol. Phys.* 3, 367
- Bogdan T. J., Carlsson M., Hansteen V. H., McMurry A., Rosenthal C. S., Johnson M., Petty-Powell S., Zita E. J., Stein R. F., McIntosh S. W., Nordlund Å., 2003, *Ap. J.* 599, 626
- Carlsson M., Stein R. F., 1992, *Ap. J.* 397, L59
- Carlsson M., Stein R. F., 1994, in M. Carlsson (ed.), *Chromospheric Dynamics*, p. 47
- Carlsson M., Stein R. F., 1997, *Ap. J.* 481, 500
- De Pontieu B., Berger T. E., Schrijver C. J., Title A. M., 1999, *Sol. Phys.* 190, 419
- De Pontieu B., Erdélyi R., de Wijn A. G., 2003a, *Ap. J.* 595, L63
- De Pontieu B., Erdélyi R., James S. P., 2004, *Nature* 430, 536
- De Pontieu B., Hansteen V. H., Rouppe van der Voort L., van Noort M., Carlsson M., 2007, *ApJ* 655, 624
- De Pontieu B., Tarbell T., Erdélyi R., 2003b, *Ap. J.* 590, 502
- Handy B. N., Acton L. W., Kankelborg C. C., Wolfson C. J., Akin D. J., Bruner M. E., Carvalho R., Catura R. C., Chevalier R., Duncan D. W., Edwards C. G., Feinstein C. N., Freeland S. L., Friedlaender F. M., Hoffmann C. H., Hurlburt N. E., Jurcevich B. K., Katz N. L., Kelly G. A., Lemen J. R., Levay M., Lindgren R. W., Mathur D. P., Meyer S. B., Morrison S. J., Morrison M. D., Nightingale R. W., Pope T. P., Rehse R. A., Schrijver C. J., Shine R. A., Shing L., Strong K. T., Tarbell T. D., Title A. M., Torgerson D. D., Golub L., Bookbinder J. A., Caldwell D., Cheimets P. N., Davis W. N., Deluca E. E., McMullen R. A., Warren H. P., Amato D., Fisher R., Maldonado H., Parkinson C., 1999, *Sol. Phys.* 187, 229
- Hansteen V. H., De Pontieu B., Rouppe van der Voort L., van Noort M., Carlsson M., 2006, *ApJ* 647, L73
- Scharmer G. B., Bjelksjö K., Korhonen T. K., Lindberg B., Petterson B., 2003, in *Innovative Telescopes and Instrumentation for Solar Astrophysics*. eds. S.L. Keil & S.V. Avakyan. *Proc. SPIE.*, Vol. 4853, p. 341
- van Noort M., Rouppe van der Voort L., Löfdahl M. G., 2005, *Sol. Phys.* 228, 191